

Theoretical description of the colossal entropic magnetocaloric effect: Application to MnAsP. J. von Ranke,^{1,*} Sergio Gama,² A. A. Coelho,² A de Campos,² A. Magnus G. Carvalho,²
F. C. G. Gandra,² and N. A. de Oliveira¹¹*Instituto de Física, Universidade do Estado do Rio de Janeiro—UERJ, Rua São Francisco Xavier, 524, 20550-013 Rio de Janeiro, RJ, Brazil*²*Instituto de Física Gleb Wataghin, Universidade Estadual de Campinas—UNICAMP, Caixa Postal 6165, 13083-970 Campinas, SP, Brazil*

(Received 31 October 2005; published 19 January 2006)

We report on the theoretical investigations into the recently discovered colossal entropy change in MnAs under magnetic-field change in an isothermal process. The phenomenological model takes into account the exchange-Zeeman interactions, magnetoelastic interactions, the external pressure effect, and the magnetic-field dependence of the lattice entropy. The results show the fundamental role of the lattice entropy in the colossal entropy change for the MnAs compound. The best model parameters and their variation with pressure were determined.

DOI: 10.1103/PhysRevB.73.014415

PACS number(s): 75.30.Sg, 65.40.-b, 74.25.Ha, 75.40.Cx

I. INTRODUCTION

Magnetic refrigeration is based in the magnetocaloric effect, which is the material ability of cooling when it is removed from the external magnetic field in an adiabatic process. Improvements in the overall magnetic refrigerator performance are critically dependent on the magnetocaloric properties of magnetic refrigerant materials, and since the discovery of giant magnetocaloric effect in the $\text{Gd}_5(\text{Si}_x\text{Ge}_{1-x})_4$ alloys in 1997 by Pecharsky and Gschneidner,¹ much scientific effort has been devoted into the investigation of the magnetocaloric effect. More recently, different giant magnetocaloric materials were reported, e. g., $\text{MnAs}_{1-x}\text{Sb}_x$,^{2,3} $\text{MnFeP}_{0.45}\text{As}_{0.55}$, and $\text{La}(\text{Fe}_{1-x}\text{Si}_x)$ and its hydrides.⁴⁻⁶ Theoretical progress, based on the Bean and Rodbell model (which predicts a first-order magnetic phase transition when the Curie temperature is strongly dependent on lattice deformation) were performed in order to understand the giant magnetocaloric behavior in $\text{Gd}_5(\text{Si}_x\text{Ge}_{1-x})_4$,⁷ $\text{MnAs}_{1-x}\text{Sb}_x$,⁸ and $\text{MnFeP}_{0.45}\text{As}_{0.55}$.⁹

The heating and cooling of any refrigerant material are connected to the entropy change associated with an external, controlled parameter change, and for a given refrigerant material, a high-entropy change occurs in the temperature range where the external parameter has stronger influence on the order-disorder transition as stated by the second law of thermodynamics. In the case of magnetocaloric materials, the external parameter is the magnetic field, the order-disorder parameter is the magnetization, and around the Curie temperature the peak occurs in the isothermal magnetic entropy change, ΔS . For magnetic materials that present discontinuity in the magnetization (first-order magnetic phase transition, high magnetic entropy change is expected, as is the case of the giant magnetocaloric materials mentioned earlier. Similar to magnetocaloric effect, some materials present isothermal entropy and adiabatic temperature changes under changing of pressure (the controlled external parameter), the so-called barocaloric effect.¹⁰ Müller *et al.*¹¹ investigated the cooling by application of pressure in the vicinity

of a pressure-induced structural phase transition in $\text{Pr}_{0.66}\text{La}_{0.34}\text{NiO}_3$. This material presents a rhombohedral to orthorhombic phase transition around $T=361$ K, leading to a different crystalline electrical field (CEF) levels scheme, and therefore, to different entropy associated with the CEF levels scheme. The role of pressure, in this material, is to enhance the fraction of rhombohedral symmetry at the expense of the fraction of the orthorhombic one, leading to entropy change and, therefore, to the sample cooling. The influence of CEF on the magnetocaloric effect was vastly investigated in rare-earth compounds, such as $(\text{Dy}_{1-x}\text{Er}_x)\text{Al}_2$,¹² YbAs ,¹³ and PrNi_5 .^{14,15} In these materials, experimental results showed an anomalous magnetocaloric effect, which was explained in the framework of the CEF theory.

The hydrostatic pressure influence on the giant magnetocaloric compound Gd_5Ge_4 was investigated by Magen *et al.*,¹⁶ measuring linear thermal expansion and magnetization isotherms at selected applied pressures. The effect of pressure is to induce a three-dimensional ferromagnetic order in Gd_5Ge_4 because of the reduction of the interatomic distances and therefore inducing the formation of the orthorhombic O(I)-type structure at the expense of the fraction of orthorhombic O(II)-type structure (in which the Gd_5Ge_4 crystallizes).

An early experimental improvement in magnetocaloric material under pressure was reported by Morellon *et al.* in $\text{Tb}_5\text{Si}_2\text{Ge}_2$ by means of thermal expansion, magnetization, and neutron powder diffraction experiments under hydrostatic pressure.¹⁷ The influence of the pressure on the $\text{Tb}_5\text{Si}_2\text{Ge}_2$ is to increase the Curie temperature at a rate faster than the rate of a crystallographic transition, so that above a critical pressure, $P_c \sim 8.6$ kbar, a coupled magnetic-crystallographic transition occurs, i.e., a monoclinic-paramagnetic to orthorhombic-ferromagnetic first-order phase transition takes place. Below the critical pressure, the magnetic phase transition uncouples from the crystallographic one and the paramagnetic-ferromagnetic transition occurs as a second-order phase transition on cooling. When a hydrostatic pressure is applied in $\text{Tb}_5\text{Si}_2\text{Ge}_2$, the peak in the

magnetic entropy change increases from 13.4 J/kg K (at $P=0$ kbar) to 22.1 J/kg K (at 10.2 kbar) for a magnetic field change of $\Delta H=5$ T. This increase in the entropy change was shown to arise from the latent heat of the crystallographic transition as predicted by Pecharsky *et al.*¹⁸

In this paper, we theoretically investigate the origin of the recent discovered colossal magnetocaloric effect (CMCE) in MnAs under hydrostatic pressure.¹⁹ The magnetocaloric effect measurements ΔS in MnAs were performed using the magnetization method, placing the MnAs sample in a proper pressure cell. The effect of the pressure is to decrease the MnAs Curie temperature and increase the ΔS peak until a critical pressure ($P_c=2.23$ kbar) and, beyond this P_C value, the CMCE effect starts to diminish. The maximum value of the entropic CMCE reaches a peak value of $\Delta S=267$ J/(kg K) (at $P_C=2.23$ kbar and $T=281$ K), which is 7.3 times greater than the value for the optimally prepared giant magnetocaloric material $\text{Gd}_5\text{Si}_2\text{Ge}_2$, (36.4 J/kg K) at $T_C=272$ K), for a magnetic-field change of $\Delta H=5$ T.²⁰ The colossal $\Delta S=267$ J/(kg K) value is far above the upper limit for the (magnetic) entropy variation value, namely, $R \ln(2J+1)$, based on the hypothesis of magnetic-field independence of the lattice and electronic contributions to the entropy. It is also not possible to explain the colossal effect as being due to the latent heat of the coupled crystallographic transition of MnAs, once this contribution is far below the measured ΔS values. The first model used to describe the magnetic state of the MnAs, which takes into account the first-order magnetic phase transition because of the strong magnetoelastic interaction, was proposed by Bean and Rodbell.²¹ In order to explain the CMCE effect, we extended the Bean and Rodbell assumption of the Curie temperature dependence on lattice deformation, considering, in addition, the Debye temperature dependence on lattice deformation through the Grüneisen model parameters. The experimental results of the CMCE effect were adjusted for different applied pressures, and the best model parameters were determined.

The model parameters are dependent on the maximum entropy variation at each fixed pressure, and from the first application of the model, it was evident that the value for ambient pressure was far from the average behavior of the parameters obtained for the other pressures. For this reason, we repeated the ΔS determination at ambient pressure, but using finer temperature and field variations, and were able to verify that the entropy effect is far greater than the value previously reported (as can be seen in Fig. 1) and greater than the magnetic limit, 103 J/(kg K). We used this new data for determining the values of the parameters of the modified Bean and Rodbell model, as described below.

II. THEORY

The Gibbs free energy, for a ferromagnetic system described by exchange interaction, under the molecular field approximation, Zeeman effect, and distortion is given by

$$G = -\frac{3}{2} \left(\frac{J}{J+1} \right) N k_B T_C \sigma^2 - H g \mu_B J N \sigma + \frac{1}{2K} \omega^2 + P \omega - TS. \quad (1)$$

In Eq. (1) J is the ion total angular momentum in the lattice, N is the number of magnetic ions per unit volume, k_B is the

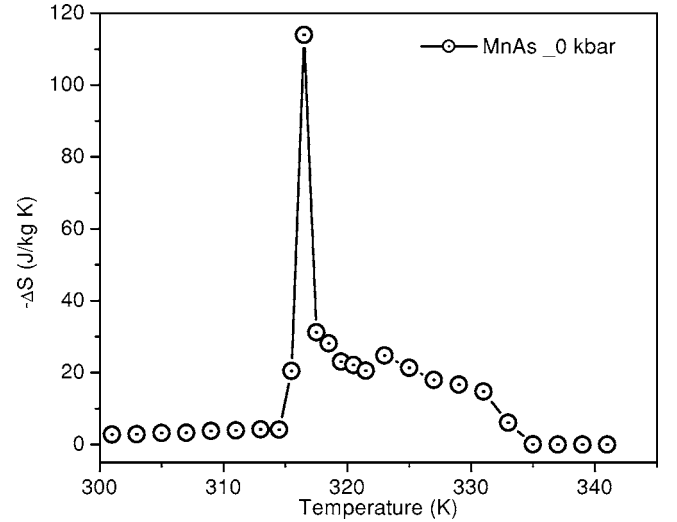


FIG. 1. Magnetocaloric effect for MnAs at room pressure measured with a finer temperature and magnetic field intervals.

Boltzmann's constant, μ_B is the Bohr magneton, $\sigma = M/g\mu_B JN$ is the normalized magnetization at absolute temperature T , g is the Landè factor, H is the external magnetic field, K is the compressibility, P is the pressure, and S is the total magnetic entropy of the system. We neglected other entropy contributions in the relation (1) since the main conclusion may be drawn from this simplified form.

The model considers the dependence of the exchange interaction on the interatomic distance. This dependence is phenomenologically described by considering the dependence of the critical magnetic phase-transition temperature on the volume change in the following way:^{21,22}

$$T_C = T_0(1 + \beta\omega). \quad (2)$$

Here $\omega = (V - V_0)/V_0$ is the cell deformation, β measures the slope of the critical temperature curve on the cell deformation, and T_0 is the order temperature in the absence of the deformation. The above free energy minimizes under the deformation

$$\omega = \frac{3}{2} \frac{J^2}{J(J+1)} N K k_B T_0 \beta \sigma^2 - PK. \quad (3)$$

Substituting the above equilibrium deformation into relation (1) and performing the derivative with respect to σ , the magnetic state equation is obtained.

$$\sigma = B_J(Y) \quad (4)$$

with

$$Y = \frac{1}{T} \left[3T_0 \left(\frac{J}{J+1} \right) \sigma + \left(\frac{g\mu_B J}{k_B} \right) H + \frac{9}{5} \left(\frac{(2J+1)^4 - 1}{[2(J+1)]^4} \right) T_0 \eta \sigma^3 - 3 \left(\frac{J\beta PK}{J+1} \right) T_0 \sigma \right], \quad (5)$$

and

$$\eta = \frac{5}{2} \frac{[4J(J+1)]^2}{[(2J+1)^4 - 1]} Nk_B K T_0 \beta^2, \quad (6)$$

where B_J is the Brillouin function. The last two terms in the argument of the Brillouin function come from the elastic deformation. The parameter η controls the order of magnetic phase transition.⁷

The magnetic entropy can be obtained from the usual relation

$$S_{\text{mag}}(T, H, P; T_0, \eta) = R \left[\ln(Z) + T \frac{\partial \ln(Z)}{\partial T} \right], \quad (7)$$

where R is the gas constant and $Z = \sinh[(2J+1)Y/2J] / \sinh[Y/2J]$.

The lattice entropy is considered in the Debye approximation

$$S_{\text{lat}}(T) = -3R \ln \left[1 - \exp\left(-\frac{\Theta_D}{T}\right) \right] + 12R \left(\frac{T}{\Theta_D} \right)^3 \int_0^{\Theta_D/T} \frac{x^3 dx}{\exp(x) - 1}, \quad (8)$$

where Θ_D is the Debye temperature. The influence of the pressure and magnetoelastic effect on the lattice entropy is obtained using the Grüneisen relation^{23,24} defined by

$$\frac{\Delta \Theta_D}{\Theta_D^0} = \frac{\Theta_D' - \Theta_D^0}{\Theta_D^0} = -\gamma \omega. \quad (9)$$

In this equation, γ is the Grüneisen parameter. Here, $\Theta_D = \Theta_D'(\sigma, P) + C$ is the Debye temperature at pressure P and magnetization σ . The introduced constant C gives the suitable boundary condition, i.e., at low temperature ($\sigma=1$) and without external pressure we chose $\Theta_D = \Theta_D^0$. In this way, the pressure and magnetization dependence of the Debye temperature is given by

$$\Theta_D = \Theta_D^0 \left[1 + \gamma \left(\frac{3}{2} \frac{J^2}{J(J+1)} Nk_B T_0 \beta (1 - \sigma^2) + KP \right) \right] \quad (10)$$

The total entropy is given by $S_T(T, P, H) = S_{\text{mag}} + S_{\text{lat}}$, and the other contributions to the total entropy of the magnetic system will be neglected. The isothermal and isobaric entropy changes ΔS_T , which occur for changes in the external magnetic field, can be directly determined

$$\Delta S_T(T, P) = S_T(T, P, H_2) - S_T(T, P, H_1). \quad (11)$$

The temperature, pressure, and magnetic-field dependence of the total entropy is not trivial, since for a given set of model parameters (T_0, β) , the magnetic state equation $\sigma = \sigma(T, H, P, \sigma)$, relation (4), must be solved self-consistently.

III. RESULTS AND DISCUSSIONS

The model parameter $T_0=285$ K was previously estimated for MnAs,²¹ the compressibility, $K=4.55 \times 10^{-12}$ (dyn/cm²)⁻¹,²⁵ and the number of particles per unit

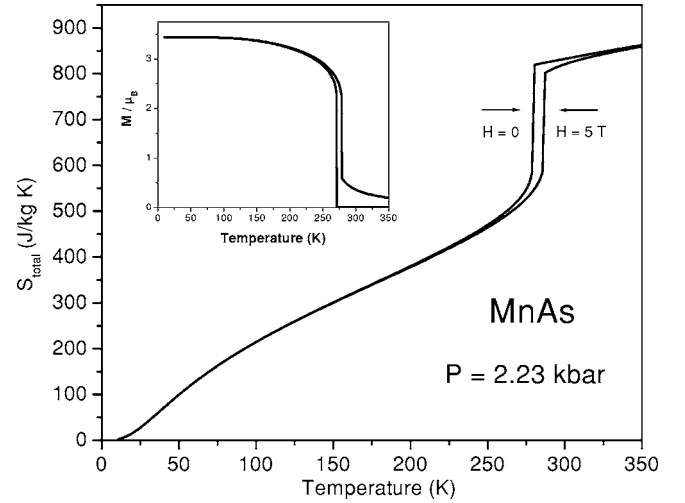


FIG. 2. Temperature dependence of total entropy for MnAs, under pressure $P=2.23$ kbar, in zero field and in applied field of 5 T. The inset shows the magnetization vs temperature.

volume $N=2.9 \times 10^{22}$ cm⁻³, taken from Ref. 21, were considered in this work. Entering with $g=2$, $J=1.72$, $\beta=13.2$, and pressure $P=2.23$ kbar into relation (6), we get $\eta=1.98$ (this η value leads the magnetic system to order under first-order ferro-paramagnetic phase transition

Using the above parameters in the magnetic state equation, relation (4), the temperature dependence of magnetization was obtained and is displayed in the inset of Fig. 2. The sharp first-order transition appears at critical temperature, $T_C=271$ K for zero magnetic field, and for $H=5$ T a shift to $T_C=278.8$ K is observed.

The Debye temperature slowly decreases with temperature until T_C , when an abrupt decrease occurs due to the coupled magnetodeformation interaction under first-order magnetic phase transition. The total entropy curves, i.e., the magnetic plus lattice entropy versus temperature with $H=0$ and $H=5$ T are plotted in Fig. 2. The colossal increases in the total entropy at T_C (of about 100 J/kg K) are due to the two combined and superimposed effects: (i) the large increase in the magnetic entropy that occurs when the ordered (ferromagnetic state) goes to the disordered (paramagnetic state) in a first-order process and (ii) the abrupt decrease in the Debye temperature at T_C , which leads to an abrupt increase of the lattice entropy. We emphasize that such total entropy variation is too great to be accounted for by the latent heat associated with the first-order transition.

We apply the above model to the experimental data of ΔS_T versus temperature in MnAs (Ref. 19) for a magnetic-field change from $H=0$ to $H=5$ T under several hydrostatic pressures, namely, $P=0, 1.13, 2.23, 2.64$ kbar. In Fig. 3, the experimental data (open circles) and the theoretical calculations (solid lines) are displayed. The two model parameters, γ and β , determined for each corresponding pressure are shown in Table I, calculated for other values of the pressure as well. The η values that appear in the last column come from relation (6), and in all cases, we obtain $\eta > 1$, which leads to the first-order magnetic phase transition. Note that the parameter values in the sixth row, for $P=2.23$ kbar, are

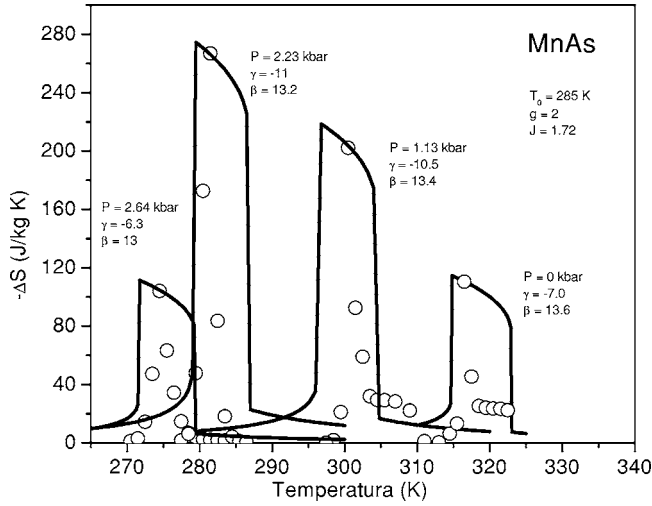


FIG. 3. Temperature dependence of total entropy changes for MnAs for a magnetic-field change from 0 to 5 T. The full lines represent the theoretical results, and the circles represent the experimental data.

the same values used to construct the curves in Fig. 2. The β parameters, determined by adjusting the experimental data, slowly increase linearly when the pressure decreases, at a rate of -0.42 kbar^{-1} , as can be seen from Fig. 4. The increase of β leads to an increase in T_C . Nevertheless, even if we fix the β parameter, the model confirms that the pressure leads to a systematic decrease in T_C , as observed experimentally. In this way, the small linear change in β was considered to improve the fit. Figure 4 shows that the η parameter also varies linearly with the applied pressure at a rate of -0.14 kbar^{-1} . In the pressure range where the CMCE is increasing, the γ parameter also decreases linearly, at a rate of -1.74 kbar^{-1} , as shown in Fig. 4. This parameter, however, starts to increase as the CMCE starts to decrease, so that the maximum in the CMCE is accompanied by a minimum for this parameter as a function of pressure (Fig. 4). The negative γ parameter is responsible for the decrease of the Debye temperature with the applied pressure, which leads to the

TABLE I. The model parameters γ and β for MnAs for different pressures. The η parameter is determined from relation (6).

| Pressure (kbar) | γ | β | η |
|-----------------|----------|---------|--------|
| 0 | -7.0 | 13.6 | 2.16 |
| 0.38 | -7.5 | 13.6 | 2.17 |
| 0.87 | -9.7 | 13.6 | 2.17 |
| 1.13 | -10.5 | 13.4 | 2.10 |
| 1.80 | -10.5 | 13.4 | 2.10 |
| 2.23 | -11 | 13.2 | 1.98 |
| 2.46 | -10.5 | 12.0 | 1.70 |
| 2.64 | -6.3 | 13.0 | 1.98 |

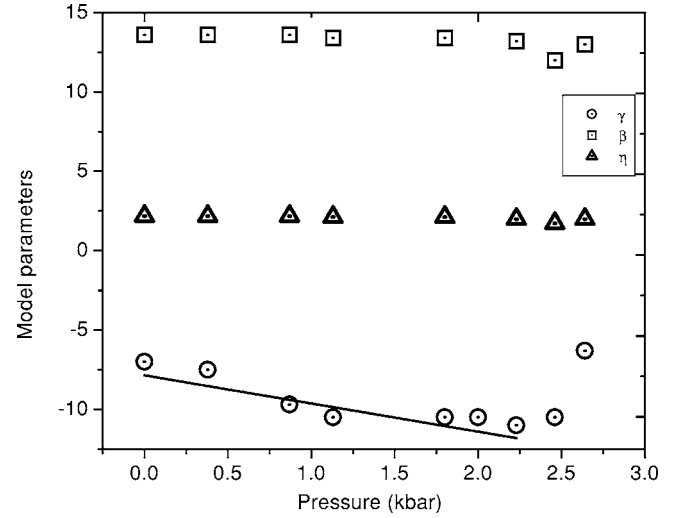


FIG. 4. Variation of the model parameters with pressure.

increase in lattice entropy. Therefore, the higher the modulus of γ is, the higher will be the peak in the ΔS_T versus temperature curve. As pressure increases, the CMCE starts to decrease steeply, following the transition observed for the Mn ion from a high- to low-spin state observed for this pressure range. The γ parameter varies accordingly to reproduce these results. We note that the model reproduces the transition temperatures and the maximum values for the CMCE well, but not the shape of the curves, indicating the model needs improvements to better reproduce the experimental data.

IV. CONCLUSION

Considering the total entropy dependence on the volumetric deformation, which changes with magnetization, external magnetic field, and pressure, it was possible to explain the origin of the colossal magnetocaloric effect in MnAs under hydrostatic pressure. The model reproduces the systematic decrease of the Curie temperature very well with the pressure as measured in MnAs, as well as the observed values of the colossal effect measured for this compound. The best model parameters were determined adjusting the ΔS_T for several pressures. The variation of the model parameters with pressure are also obtained from the fittings to the experimental data.

ACKNOWLEDGMENTS

We acknowledge financial support from CNPq—Conselho Nacional de Desenvolvimento Científico e Tecnológico—Brazil, CAPES—Coordenação de Aperfeiçoamento de Pessoal de Nível Superior—Brazil, FAPERJ—Fundação de Amparo à Pesquisa do Estado do Rio de Janeiro and FAPESP—Fundação de Amparo à Pesquisa do Estado de São Paulo. This work was also partially supported by PRONEX Grant No. E-26/171.168/2003 from FAPERJ/CNPq. We are also grateful to Dr. Thierry Strässle for sending us his Ph.D. thesis.

*Electronic address: vonranke@nitnet.com.br

- ¹V. K. Pecharsky and K. A. Gschneidner, Jr., *Phys. Rev. Lett.* **78**, 4494 (1997).
- ²H. Wada and Y. Tanabe, *Appl. Phys. Lett.* **79**, 3302 (2001).
- ³H. Wada, T. Morikawa, K. Taniguchi, T. Shibata, Y. Yamada, and Y. Akishige, *Physica B* **328**, 114 (2003).
- ⁴O. Tegus, E. Brück, K. H. J. Buschow, and F. R. de Boer, *Nature (London)* **415**, 150 (2002).
- ⁵F. Hu, B. Shen, J. Sun, Z. Cheng, G. Rao, and X. Zhang, *Appl. Phys. Lett.* **78**, 3675 (2001).
- ⁶A. Fujita, S. Fujieda, Y. Hasegawa, and K. Fukamichi, *Phys. Rev. B* **67**, 104416 (2003).
- ⁷P. J. von Ranke, N. A. de Oliveira, and S. Gama, *J. Magn. Magn. Mater.* **277**, 78 (2004).
- ⁸P. J. von Ranke, N. A. de Oliveira, and S. Gama, *Phys. Lett. A* **320**, 302 (2004).
- ⁹P. J. von Ranke, A. de Campos, L. Caron, A. A. Coelho, S. Gama, and N. A. de Oliveira, *Phys. Rev. B* **70**, 094410 (2004).
- ¹⁰Th. Strässle, Ph.D. thesis, Swiss Federal Institute of Technology ETH, Zürich, 2002 (unpublished).
- ¹¹K. A. Müller, F. Fauth, S. Fischer, M. Koch, A. Furrer, and Ph. Lacorre, *Appl. Phys. Lett.* **73**, 1056 (1998).
- ¹²A. L. Lima, I. S. Oliveira, A. M. Gomes, and P. J. von Ranke, *Phys. Rev. B* **65**, 172411 (2002).
- ¹³P. J. von Ranke, A. L. Lima, E. P. Nobrega, X. A. de Silva, A. P. Guimarães, and I. S. Oliveira, *Phys. Rev. B* **63**, 024422 (2001).
- ¹⁴P. J. von Ranke, V. K. Pecharsky, K. A. Gschneidner, and B. J. Korte, *Phys. Rev. B* **58**, 14436 (1998).
- ¹⁵P. J. von Ranke, M. A. Mota, D. F. Grangeia, A. M. Carvalho, F. C. G. Gandra, A. A. Coelho, A. Caldas, N. A. de Oliveira, and S. Gama, *Phys. Rev. B* **70**, 134428 (2004).
- ¹⁶C. Magen, Z. Arnold, L. Morellon, Y. Skorokhod, P. A. Algarabel, M. R. Ibarra, and J. Kamarad, *Phys. Rev. Lett.* **91**, 207202 (2003).
- ¹⁷L. Morellon, Z. Arnold, C. Magen, C. Ritter, O. Prokhnenko, Y. Skorokhod, P. A. Agarabel, M. R. Ibarra, and J. Kamarad, *Phys. Rev. Lett.* **93**, 137201 (2004).
- ¹⁸V. K. Pecharsky, A. P. Holm, K. A. Gschneidner, Jr., and R. Rink, *Phys. Rev. Lett.* **91**, 197204 (2003).
- ¹⁹S. Gama, A. A. Coelho, A. de Campos, A. M. Carvalho, F. C. G. Gandra, P. J. von Ranke, and N. A. de Oliveira, *Phys. Rev. Lett.* **93**, 237202 (2004).
- ²⁰A. O. Pecharsky, K. A. Gschneidner, Jr., and V. K. Pecharsky, *J. Appl. Phys.* **93**, 4722 (2003).
- ²¹C. P. Bean and D. S. Rodbell, *Phys. Rev.* **126**, 104 (1962).
- ²²D. S. Rodbell, *Phys. Rev. Lett.* **7**, 1 (1961).
- ²³E. Grüneisen, *Ann. Phys.* **39**, 257 (1912).
- ²⁴J. S. Dugdale and D. K. C. MacDonald, *Phys. Rev.* **89**, 832 (1953).
- ²⁵N. Menyuk, J. A. Kafalas, K. Dwight, and J. B. Goodenough, *Phys. Rev.* **177**, 942 (1969).